# Hydrological Signals in Height and Gravity in Northeastern Italy inferred from Principal Components Analysis

S. Zerbini, F. Raicich, B. Richter, V. Gorini, M. Errico

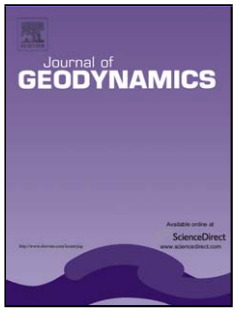


Title: Hydrological Signals in Height and Gravity in Northeastern Italy inferred from Principal Components Analysis

Authors: S. Zerbini, F. Raicich, B. Richter, V. Gorini, M. Errico

PII: S0264-3707(09)00152-5
DOI: doi:10.1016/j.jog.2009.11.001
Reference: GEOD 950

To appear in: *Journal of Geodynamics*

Received date: 23-1-2009
Revised date: 28-10-2009
Accepted date: 10-11-2009

Please cite this article as: Zerbini, S., Raicich, F., Richter, B., Gorini, V., Errico, M., Hydrological Signals in Height and Gravity in Northeastern Italy inferred from Principal Components Analysis, *Journal of Geodynamics* (2008), doi:10.1016/j.jog.2009.11.001

# Hydrological Signals in Height and Gravity in Northeastern Italy inferred from Principal Components Analysis

**S. Zerbini[a,*], F. Raicich[b], B. Richter[c], V. Gorini[a], M. Errico[a]**

[a] *Dipartimento di Fisica, Università di Bologna,Viale Berti Pichat 8, I-40127 Bologna, Italy*
[b] *CNR-Istituto di Scienze Marine, Sede di Trieste, V.le Romolo Gessi 2, I-34123, Trieste,Italy*
[c] *Bundesamt fuer Kartographie und Geodaesie, Richard-Strauss-Allee 11, D-60598 Frankfurt am Main, Germany*

## Abstract

This work describes a study of GPS heights, gravity and hydrological time series collected by stations located in northeastern Italy. During the last 12 years, changes in the long-term behaviors of the GPS heights and gravity time series are observed. In particular, starting in 2004-2005, a height increase is observed over the whole area. The temporal and spatial variability of these parameters has been studied as well as those of key hydrological variables, namely precipitation, hydrological balance and water table by using the Empirical Orthogonal Functions (EOF) analysis. The coupled variability between the GPS heights and the hydrological balance and precipitation data has been investigated by means of the Singular Value Decomposition (SVD) approach. Significant common patterns in the spatial and temporal variability of these parameters have been recognized. In particular, hydrology-induced variations are clearly observable starting in 2002-2003 in the southern part of the Po Plain for the longest time series, and from 2004-2005 over the whole area. These findings, obtained by means of purely mathematical approaches, are supported by sound physical interpretation suggesting that the climate-related fluctuations in the regional/local hydrological regime are one of the main

* Corresponding author.
*E-mail address:* susanna.zerbini@unibo.it

contributors to the observed variations. A regional scale signal has been identified in the GPS station heights; it is characterized by the opposite behavior of the southern and northern stations in response to the hydrological forcing. At Medicina, in the southern Po Plain, the EOF analysis has shown a marked common signal between the GPS heights and the Superconducting Gravimeter (SG) data both over the long and the short period.

*Keywords:* GPS height; gravity; hydrology; subsidence; Empirical Orthogonal Functions; Singular Value Decomposition method

## 1.0 Introduction

The long (multi year) and short (seasonal to a few years) period oscillations observed in the continuous time series of GPS heights and gravity result from the superimposition of various phenomena of different physical nature. Among them, tectonics and the mass transport in the Earth's system which induces deformation of the Earth's crust in response to variations of the load due to hydrology, air pressure and non-tidal oceanic effects. Continuous GPS time series exceeding a decade are now available which can provide reliable information on the long-term height evolution (linear and non-linear) as well as on the short-period seasonal fluctuations. However, it is complicated to unravel the contribution of the different components in the observed long-term height behavior because, at global scale, the Glacial Isostatic Adjustment (GIA) is the only coherent geological contribution to height variation for which understanding of the physical process has been achieved. Superconducting gravimeter and/or absolute gravity

measurements are not as widely spread as those of GPS, but where both types of measurements are available, they offer a unique means to detect and understand mass contributions.

It was shown that hydrological mass variations play a major role in the seasonal height and gravity variability (van Dam et al., 2001; Zerbini et al., 2007). On long-time scales, climate-related variations of GPS heights and gravity have not yet been clearly identified mainly because of the limited temporal extent of most of the continuous series and for the lack of information on the spatial and temporal variability of groundwater storage.

We have studied the variations observed during the last decade in the GPS heights, gravity and the hydrological time series in northeastern Italy (Fig. 1), as well as their mutual relationships. The investigated area is affected by both natural and human-induced subsidence. The Po Plain is a subsiding sedimentary basin encompassed by the Alps, Apennines and Dinarides Chains. Two structural environments occur within the basin: the north-verging Apennine fold-and-thrust belt system that is buried under the Plio–Quaternary cover and a platform gently dipping from the Alps into the basin (Carminati and Martinelli, 2002). Sedimentation has filled the basin with alternate stratigraphic sequences of sands, silts and clays variably interbedded and normally consolidated and containing water in the form of impregnating water and groundwater (Zerbini et al., 2000; 2002). These conditions are most favorable for the development of both natural and anthropogenic subsidence. Long-term natural subsidence rates range between 1-to-2 mm/yr (Pignone et al., 2008), with maximum rates of 2.5 mm/yr evaluated from the analysis of borehole stratigraphies and from available seismic sections

(Carminati et al., 2003) with the largest rates occurring in the southern part of the Po Plain and in the Po Delta. As discussed by Carminati and Di Donato (1999), backstripping analysis suggests that tectonics accounts for about 50% of the long-term natural subsidence, whereas compaction and sediment load account for about 30 and 20%, respectively. However, the present-day geodetic observations show subsidence rates with peaks up to 40 mm/yr resulting from an anthropogenic component superimposed to the natural subsidence. The anthropogenic contribution has been generated by systematic exploitation of groundwater for both industrial and civil use for about 50 years starting during 1950s. Groundwater control policies have been adopted since the beginning of the 1980s with the consequent reduction of fluids withdrawal.

In our study, we have adopted the Empirical Orthogonal Functions (EOF) and the Singular Value Decomposition (SVD) analyses. Significant common patterns in the spatial and temporal variability of GPS heights, gravity and hydrological parameters have been identified. In particular, hydrology-induced variations are clearly observable starting in 2002-2003 in the southern part of the Po Plain for the longest GPS time series as well as for gravity, and from 2005 for the GPS heights over the whole area. Observing and modeling long- and short-period signals in the height and gravity time series allows to better understand and quantify subsidence. This knowledge is important because of the relevant societal impacts of this phenomenon.

## 2.0 Data

In northeastern Italy, several data sets are available that can be used for a spatial/temporal analysis of potentially common signals. These are time series of GPS heights, hydrological information, such as precipitation, simplified hydrological balance (precipitation minus evapotranspiration) and water table data, and series of absolute gravity and superconducting gravimeter measurements. Four of the GPS time series are rather long (about a decade or longer) and continuous.

**2.1 GPS**

We have used the continuous GPS data of a network located in northeastern Italy (Fig. 1 and Table 1). The observations were analyzed by means of the Bernese software package version 5.0 (Dach et al., 2007). The data were processed by using high-accuracy International GNSS Service (IGS) products including the ionospheric files, the satellite orbits and the Earth rotation parameters. The ITRF2005 coordinates and velocity field (Altamimi et al., 2007) were adopted for five IGS stations in Europe (ZIMM, GRAZ, MEDI, MATE and CAGL) used as fiducial sites in the network adjustment procedure. In Medicina, there are two GPS receivers, MEDI and MSEL, installed at a distance of about 30 m from each other. Both MEDI and MSEL are EUREF EPN stations. One important aspect is that the antennas/receivers of the stations, except for MEDI, were never substituted during the time period of the present analysis. This ensures a desirable homogeneity of the height series and the absence of jumps due to ~~a~~ change of instrumentation. The MEDI height time series presented in this paper for comparison purposes is a EUREF solution kindly provided by K. Szafranek and A. Kenyeres (2009).

120

121 **2.2 Hydrology**

122

123 For all stations, we have estimated a simplified daily hydrological balance. The data
124 used were the daily precipitation and maximum and minimum air temperature to derive
125 estimates of the potential evapotranspiration according to the Hargreaves equation
126 (Hargreaves and Samani, 1982, 1985). In addition, at Medicina, continuous
127 measurements of the surficial water table are available.

128 In order to compare the hydrological balance data with those of GPS heights and
129 gravity, we have built hydrological time series in which the n-th element is the time
130 integral of the daily values from 1 (first epoch) to n. The linear trends have been removed
131 from these time series in order to highlight the seasonal to interannual variability of the
132 local hydrology. The residuals turn out to be useful proxies for the surficial water table
133 fluctuations. Precipitation, treated in the same way as the hydrological balance, also
134 appears to be a good proxy for the multi-year behavior of the water table. The
135 identification of reliable proxies is necessary because water table data are not, in general,
136 readily available. Figure 2 illustrates, as an example for the Medicina station, a
137 comparison between hydrological balance, precipitation and water table data residuals.
138 The three series are in good agreement as regards the long-term behavior and the phase of
139 the seasonal cycle. However, the amplitude of the oscillations of the water table is not
140 always well represented by the hydrological balance and precipitation.

141

142 **2.3 Gravity**

Superconducting gravimeter (SG) and absolute gravity (AG) observations are performed at Medicina, while in Loiano, Bologna, Voltabarozzo, Marghera, Cavallino and Treviso only AG measurements are carried out (Table 1). The continuous SG measurements at Medicina start at the beginning of 1998. An instrumental linear drift (18.6 $nms^{-2}$/yr) was estimated by comparison with a series of AG measurements performed by means of FG-5 instruments. The gravity data have been analyzed according to the description given in Zerbini et al. (2007).

## 3.0 Methods: EOF and SVD analyses

Our objective is twofold: we aim at recognizing both spatial and temporal variability patterns. We will study the behaviour of individual variables, namely GPS height, gravity, precipitation, hydrological balance and water table and of variable pairs, for example, GPS height and precipitation. The analysis is performed using a principal component approach.

In particular, following the terminology proposed by Björnsson and Venegas (1997) and Venegas (2001), the EOF method is used to analyse individual variables and the SVD method for variable pairs. It should be mentioned that the terminology is not univocal in the literature. The EOF and SVD techniques are widely used in geophysics to analyse temporally and spatially varying fields allowing transforming the data into a different set with some desirable properties (for more details, see Bretherton et al. (1992),

165 von Storch and Navarra (1999), Björnsson and Venegas (1997), Venegas (2001) and
166 Hannachi (2004)).

167 The variability of geophysical fields is the result of complex nonlinear interactions
168 between very many degrees of freedom, and a challenging task is to discriminate between
169 signal and noise. The definition of signal and noise depends on the specific object of
170 interest, but, in general, the signal can be a pattern in space and/or time, while the noise,
171 physical or instrumental, consists of features that are not relevant for the signal.
172 Normally, the signal has larger temporal and spatial scales and fewer degrees of freedom
173 than the noise.

174 The EOF analysis provides a compact description of the temporal and spatial
175 variability of a data set of a single variable in terms of orthogonal components or, also
176 called, statistical "modes". Conceptually, the decomposition in EOFs is analogous to,
177 e.g., those in Fourier periodic functions or Legendre polynomials. The difference is that
178 the EOF basis functions are not analytic but empirical; the members are not chosen on
179 analytical considerations, but on maximization of the data projection on them. The first
180 EOF is selected to be the pattern on which the data project most strongly. In other words,
181 the leading EOF is the pattern most frequently realized. The second mode is the one most
182 commonly realized under the constraint of orthogonality to the first one, the third is the
183 most frequently realized pattern that is orthogonal to both higher modes, and so on.

184 Each EOF is associated to a percentage of the total variance (PVE, percent variance
185 explained) of the original data set, which accounts for the relative importance of the
186 corresponding mode of variability. This allows recognizing dominant modes, which are
187 likely to compose the signal, leaving out the remainder, which is the noise.

Let f(x,t) be the variable of interest, defined at n locations ($x_1$,...,$x_n$) and at m times ($t_1$,...,$t_m$). The data are usually arranged in a m×n matrix (F), where each of the n columns represents the time series for a given location, and each of the m rows represents the spatial distribution at a given time. F can be written as:

$$F = U\Gamma V^T$$

$\Gamma$ is a rectangular (m×n) matrix with positive or zero elements on the diagonal ($\gamma_k$, k=1,….., min(m,n)) and zeroes elsewhere. U is a (m×m) quadratic matrix, whose columns ($u^k$) are orthogonal and represent the EOFs, (or modes or patterns, functions of space only). $V^T$ is a (n×n) quadratic matrix, whose rows ($v^{Tk}$) are also orthogonal and represent the principal components (functions of time only).

The original field can be reconstructed as a linear combination of all the modes:

$$F_m(t) = \Sigma_k \, u_m{}^k \, a_k(t)$$

where $a_k(t) = \gamma_k \, v^{Tk}(t)$. Since, in the literature, the nomenclature of the quantities involved in the analysis is not univocal, we will call $u^k$ the “spatial patterns” and $a_k$ the “time components”.

The SVD technique has the same purpose as the EOF, but each component describes a mode of coupled variability of two fields. Similarly to the EOF, each SVD is associated to a percentage of total covariance (SCP, squared covariance percentage).

The strength of the coupling for each SVD can be quantified by estimating the correlation coefficient between the relevant time components. In order to assess the

confidence level of such correlation, we need the number of independent data pairs ($N_{ind}$) involved (i.e. the number of degrees of freedom). In our case, a rigorous estimate is difficult, therefore we adopt the following definition: $N_{ind} = N_{tot}T_d / T$. Here $N_{tot}$ is the number of available data pairs, $T_d$ the "decorrelation time", namely the first zero of the time autocovariance function of the involved variables, and T the length of the time interval covered by all the data. In the present analysis, the GPS data exhibit quite larger $T_d$ values (1.2-1.3 years) than the hydrological balance does (about 0.4 years) and precipitation (about 0.5 years). As a consequence, the number of independent data pairs is approximately reduced by a factor of 20, when the hydrological balance is involved, or by a factor of 30, in the case of precipitation.

It shall be pointed out that these analyses are purely statistical; therefore the physical interpretation of the individual components requires specific arguments.

## 4.0 Linear trends: GPS height, gravity and hydrology

All stations, except Loiano, which is on the uprising chain of the Apennines, are located in the Po Plain and northeastern Adriatic; this area is characterized by relevant natural subsidence. The largest rates are mainly of anthropogenic nature (Zerbini et al., 2007). Figure 3 presents the time series of the GPS heights in the ITRF2005 and the AG and SG gravity series of the stations in the network. Gravity has been multiplied by a factor (-1) in order to facilitate the visual comparison with the height data. The height time series show a decrease in the subsidence rates starting around 2004-2005; an exception is San Felice which, instead, exhibits an increase in subsidence. Table 1 lists,

234 both for GPS and gravity, the linear trends computed over the entire time span. The
235 formal errors associated to the linear trend estimates both of GPS height and gravity have
236 been multiplied by an arbitrary factor of 5 in order to provide a conservative estimate of
237 the errors. Figure 3d concerns the Medicina station. It presents the MEDI and MSEL GPS
238 height series as well as the SG and AG gravity observations multiplied by (-1). The two
239 GPS series and those of gravity are comparable. They all show from about 2005 a
240 different long-term behavior, a reduction of subsidence, with even a tendency to uplift
241 during the last two years 2006-2007.

242 In Bologna (EUREF EPN station BOLG, Figure 3c), the linear trend turns out to be
243 -10.57±0.25 mm/yr for the period 1999-2008 and -8.31±0.40 mm/yr in the time frame
244 2002-2008 corresponding to the period for which absolute gravity measurements are also
245 available. The trend estimated from the gravity data is +4.17±1.75 μGal/yr, consistent
246 with the GPS results, within the statistical error, if using the free-air conversion factor
247 (Vaníček and Krakiwski, 1986). The free-air relation mostly occurs locally (Torge,
248 1989).

249 In the Bologna area, data acquired with the Interferometric Synthetic Aperture Radar
250 (InSAR) technique are available. In a previous work (Zerbini et al., 2007), a first
251 comparison was made between the GPS and InSAR subsidence rates which showed the
252 consistency of the two estimates. A recent analysis of InSAR observations (Ferretti,
253 T.R.E., 2009), allows a further comparison supporting the reduction in the subsidence
254 rate observed by GPS at the BOLG station. T.R.E. kindly provided us with the results of
255 their Permanent Scatterers (Ferretti et al., 2001) analysis for two different periods and
256 satellites images. Figure 4 (a) shows the InSAR results obtained using the ERS satellite

images for the period 1992-2000 and (b) the RADARSAT passes in the time frame 2003-2007. The comparison between the two images indicates a major reduction in the subsidence rate over the Bologna area in the latter period.

The stations around the Venice area (Fig. 3 f, g, h, i and j) show reasonable agreement between the GPS and AG linear trends. However, it should be pointed out that the AG series are still limited in time and the associated errors, in particular for Marghera and Cavallino, located a few hundred meters from the sea shore, are rather large.

The main hydrological parameters used in this work are the integrated simplified hydrological balances and the precipitation series as described in section 2.2. In order to achieve an understanding of the long-period behavior of the regional hydrology, we estimated the linear trend of the hydrological balance for all stations over the period 1998-2007. It was found that, over this decade, only the northern stations at Treviso (+362±4 mm/yr), Voltabarozzo (+35±3 mm/yr) and Cavallino (+38±3 mm/yr) gain water, while in all other sites, the amount of water is decreasing. In particular, the stations located in the Plain, south of the Po River (Medicina, Marina di Ravenna, Bologna and Boretto), are characterized by large negative trends up to -500 mm/yr. The analysis of the precipitation series shows similar results.

## 5.0 Long-period oscillations

Many authors have shown that short-period (seasonal) height and gravity oscillations are related to seasonal mass variations (see, for example, Blewitt et al., 2001; van Dam et

al., 2001; Zerbini et al., 2007). On the other hand, long-period (multi year) variations are not as yet well understood because of the limited length of most of the time series.

In order to identify long-period oscillations, both the GPS heights and the hydrological series were detrended to derive the residuals (Fig. 5). Possible correlations between these residuals were investigated. For the sake of clarity, we point out that we identify as hydrological balance and precipitation residuals the detrended series of the time integral values of the observed hydrological balance and precipitation respectively. Linear regressions were calculated between the height and the corresponding hydrological balance and precipitation residual values.

By considering the Marina di Ravenna and Medicina residuals (Fig. 5b and d), over the long period (multiyear), we observe anticorrelation between the height and each of the two hydrological parameters. Anticorrelation can be interpreted as the loading effect on the Earth's crust caused by the hydrology. In particular, for the MSEL station, a regression between the hydrological balance and the height residuals over the period 1996-2008 provides a ratio of −24.7±0.7 (significant at 99% confidence level), which implies that for an increase of 24.7 mm of hydrological balance there is 1 mm decrease in height (loading effect). A similar result is obtained by using the precipitation data (−18.6±0.4, 99% confidence level). At Marina di Ravenna, on the Adriatic coast, the ratios turn out to be −7.9±0.4 and −8.1±0.2 for the hydrological balance and the precipitation residuals respectively. Since this site is on the coast, the magnitude of the loading effect turns out to be smaller than that of the inland site (van Dam et al., 1994), in this case about a factor of 2-to-3 of that observed inland at Medicina. The BOLG station height residuals are characterized by a positive although weak correlation, +3.3±0.4 and

+4.1±0.2, with the hydrological balance and precipitation residuals respectively. All the northern stations exhibit positive correlation. Since correlation is not explained by loading, different physical mechanisms shall be invoked. A possible explanation could be provided by the buoyancy effect according to which an increase/decrease of the groundwater amount in the soil would produce an increase/decrease of height. Also clay swelling/shrinking on water uptake/loss may occur. The different observed behaviors can be related to the different geological settings and to the environmental conditions.

## 6.0 Regional analysis

The residual series of the GPS heights and gravity were analyzed both individually and in conjunction with hydrological parameters by means of the EOF and SVD approaches. We performed an EOF analysis on the individual variables, namely GPS height, precipitation and hydrological balance, in order to identify spatial and temporal variability features at local and regional scales. Additionally, at Medicina, the EOF analysis has been carried out between pairs of variables: GPS height and water table, gravity and hydrology, GPS height and gravity. The SVD analysis has been applied to detect common signals between GPS heights and precipitation as well as between GPS heights and hydrological balance. The length of the time series is an important factor because only three GPS stations are present for a decade or longer, while all the stations are simultaneously available only from 2004.

In order to reduce the high-frequency variability, the analysis is performed on weekly time series. The weekly values were obtained by averaging the original daily data. A

weekly mean was computed when at least four daily values were available. Gaps shorter than three days were preliminarily interpolated using the Objective Analysis technique (Gandin, 1965; Bretherton et al., 1976).

The EOF and SVD analyses require that all series be defined at the same epochs; the time series were detrended over the common period. Since variables measured in different units may be involved, all the residual time series were standardized to zero mean and unit standard deviation.

In the following, several cases were considered. Since we are interested in understanding the long-period variability observed both in the height and gravity data, only the stations with observation periods longer than six years were analyzed. We point out that the gaps in the EOFs series are mostly due to missing GPS data at the Boretto station. We will discuss spatial patterns, i.e. the coefficients shown in Tables 2 through 5 for the EOF analysis and Tables 6 and 7 for the SVD method, and time components, i.e. the curves shown in Figures 6 and 7 for the EOF and Figure 8 for the SVD. For each case, we will comment only the two largest EOFs (EOF1 and EOF2) and SVDs (SVD1 and SVD2) because, in general, they explain most of the observed variance. However, Tables 2 to 7 list the whole set of EOF and SVD spatial patterns.

**6.1 GPS height series**

*Case A - Five GPS stations (1999-2007)*

In this case, identified as case A, we analyse the GPS height time series of five stations: MSEL, MEDI, Marina di Ravenna, BOLG and Boretto. These sites are located in the southern part of the region and are characterized by the longest data records, spanning about eight years, from 1999 to the end of 2007. Concerning EOF1, the spatial pattern shows that all stations behave coherently (Table 2). A height increase is observed starting 2004-2005. A clear seasonality is superimposed with summer maxima and winter minima (Fig. 6a). The spatial pattern of EOF2 is characterized by opposite behaviours of Medicina (both MSEL and MEDI) and Boretto on one side, and Marina di Ravenna and BOLG on the other. The EOF2 time component also shows a long-term signal, the slope inversion starting around 2004.

*Case B - Eight GPS stations (2001-2007)*

Here we consider the stations of the previous case plus Cavallino, San Felice and Voltabarozzo. In this case, called case B, eight stations are simultaneously available for a period of about six years, from 2001 through the end of 2007, thus allowing us to extend the analysis to the northern part of the region. Both EOF1 and EOF2 time components show a long-term change starting around 2004-2005 (Fig. 6b). However, the EOF1 spatial pattern exhibits a different behaviour if we compare the northern and southern stations (Table 3): while the northern sites have winter height maxima, the southern ones, except BOLG, exhibit minima. Instead, the EOF2 spatial pattern is coherent across the whole region.

370 **6.2 Precipitation time series**

371

372 The two cases described previously for the GPS heights are now considered for the
373 precipitation time series. It shall be pointed out that, for the Medicina site, we deal with a
374 unique precipitation series since the two GPS receivers (MEDI and MSEL) are separated
375 by 30 m only. Moreover, for Marghera, the precipitation data are not available.
376 Therefore, we will analyze two cases with four and seven stations respectively. Both
377 analyses show that EOF1 explains at least 75% of variance.

378

379 *Four precipitation stations (1999-2007)*

380

381 The Medicina, Marina di Ravenna, Bologna and Boretto precipitation series are
382 analyzed during the period 1999-2007. These precipitation stations are identified in the
383 relevant Tables with the abbreviations ME, RA, BO and BR respectively. EOF1 is
384 characterized by a coherent spatial pattern and by significant interannual fluctuations
385 (Table 4 and Fig. 7a). Considerable precipitation minima are found in 1999, 2002, 2003
386 and 2007 and maxima during the winters 1999-2000, 2002-2003 and during most of
387 2006. In Medicina and Bologna, EOF2 exhibits a decrease until 2003-2004, followed by
388 an increase; the opposite is found in Marina di Ravenna and Boretto.

389

390 *Seven precipitation stations (2001-2007)*

391

Cavallino, San Felice and Voltabarozzo precipitation time series are considered in addition to the four stations mentioned above; in the Tables they are identified by means of the following abbreviations: CA, SF and VO respectively. The results are quite similar to those of the previous case (Table 5 and Fig. 7b).

### 6.3 Hydrological Balance time series

We analyzed also the hydrological balance time series by following the same scheme used for the precipitation data described above. EOF1s, explaining about 90% variance, are characterized by spatial coherence over the entire region. The related time components exhibit a clear seasonality. The EOF2s are comparatively much smaller than those in the case of precipitation.

### 6.4 GPS height and precipitation

The coupled variability of GPS height and hydrological variables (precipitation and hydrological balance) is studied by using the SVD approach. Within the SVD analysis we also distinguish two cases.

*Five GPS and four precipitation stations (1999-2007)*

We analyze the GPS heights of case A together with the Medicina, Marina di Ravenna, Bologna and Boretto precipitation series for the period 1999-2007. SVD1

explains 81% covariance; the precipitation spatial pattern is characterized by coherence (Table 6b). The GPS height spatial pattern is anticorrelated with precipitation at Medicina (both MSEL and MEDI) and Boretto, while RA and BOLG do not show significant correlation (Table 6a). Both time components exhibit a long-period fluctuation, with a minimum around 2003-2004 (Fig. 8a), superimposed to which are seasonal oscillations. The anticorrelation can be interpreted as a loading/unloading effect on the Earth's crust caused by variations in the precipitation regime. The SVD2 spatial pattern of the GPS height mostly exhibits regional coherence. Both time components show a long-term fluctuation with a seasonal signal superimposed. GPS is characterized by decreasing heights until beginning of 2004 and by an increase afterwards.

The correlation coefficients between the relevant SVD time components turn out to be 0.45 for SVD1 and 0.65 for SVD2, SVD1 significant at 93% confidence level while SVD2 significance is greater than 99%.

*Eight GPS and seven precipitation stations (2001-2007)*

Here we analyze the GPS heights of case B together with the seven precipitation series mentioned above. The time span thus reduces to 2001-2007. The covariance explained by SVD1 amounts to about 92%. The precipitation spatial pattern is coherent (Table 7b), while the GPS height pattern is characterized by a dipole (Table 7a). As regards the northern stations, GPS heights are correlated with precipitation, while the southern ones are anti-correlated. SVD2 shows a low percentage of covariance (6%). A long-term fluctuation is clearly recognizable in both SVDs with characteristics similar to

438 those of the previous case (Fig. 8b). Here, the correlation coefficients are 0.45 for SVD1
439 and 0.64 for SVD2, the first is significant at 90% confidence level while the significance
440 of the second is 98%.

441 Since SVD1 explains more than 90% of the signal and the GPS height pattern
442 exhibits a well-defined south-north asymmetry, we further investigated the relationship
443 between the GPS height and precipitation. After estimating the average standard
444 deviations of the two parameters for the southern and northern parts of the region
445 respectively, we have computed the relevant ratios indicative of the height response to
446 precipitation variations. In the south, the ratio turns out to be 1 mm of height for 20 mm
447 of precipitation. In the north the ratio is instead 1/35. Because, by definition, the standard
448 deviation is a positive quantity, the signs are deduced from those of the relevant SVD1
449 spatial patterns (Table 7); therefore in the south the sign of the ratio is negative whereas
450 in the north it is positive. These values are in agreement with those derived by means of
451 linear regressions between height and precipitations residuals (see section 5.0). If we
452 assume a 1 mm homogeneous increase of precipitation over the entire area, there would
453 be about 0.05 mm height decrease in the southern part while a height increase of about
454 0.03 mm would occur in the north.

455

456 **6.5 GPS height and hydrological balance**

457

458 The coupled variance between GPS height and hydrological balance exhibits results
459 quite similar to those obtained by using precipitation. In all these analyses, the SVD1s
460 explain a slightly larger covariance compared to the same cases involving precipitation.

461 The spatial patterns of the hydrological balance are always regionally coherent; however,
462 as in section 6.4, the GPS heights of the northern stations are correlated with the
463 hydrological balance, while the southern ones are anti-correlated except for BOLG.
464
465 **7.0 Local scale analysis - Medicina**
466
467 At Medicina, time series of various parameters are acquired continuously for more
468 than a decade now, GPS height (MSEL and MEDI stations), SG gravity, water table data
469 and other environmental information. This makes it possible to compare locally the
470 different series. A few examples are provided, namely we correlate, by means of the EOF
471 analysis, GPS height (both MEDI and MSEL) with water table, SG gravity with
472 precipitation and water table respectively and GPS height and SG gravity. Tables 8
473 through 10 present the pattern coefficients while the time components are presented in
474 Figures 9, 10 and 11.
475
476 **7.1 GPS height and water table**
477
478 The two GPS height data sets, MSEL and MEDI, exhibit the same response to the
479 water table variations (Fig. 9a and b, Table 8a and b). Both EOF1s are clearly
480 representative of the loading/unloading effect caused by the seasonal water table
481 variations. We observe maxima in the summer when the water table decreases and
482 minima in the winter when the water table rises close to the topographic surface. This
483 comparison also allows identifying a height decrease starting in 2002-2003 followed by a

484 height increase starting at the end of 2005. These long-period height variations are
485 correlated with increase/decrease in the water table level as a consequence of changes in
486 the precipitation regime.
487
488 **7.2 SG gravity and hydrology**
489
490 We have compared the SG data series with those of precipitation and water table. The
491 results provided by the two cases are similar (Fig. 10a and b; Table 9a and b), although
492 the SG data are slightly more correlated with the water table variations (63.6% PVE) than
493 to those of precipitation (52.7% PVE). Both EOF1s show a clear seasonal signal with
494 summer minima and winter maxima likely resulting from the combination of two effects:
495 the variations in gravity due to the Newtonian mass attraction and to height fluctuations.
496 In fact, the EOF1s pattern coefficients have the same sign indicating on the one hand that
497 to an increase/decrease of water mass corresponds an increase/decrease of gravity; on the
498 other hand an increase of water/precipitation will load the crust inducing a height
499 decrease, which turns into a gravity increase. In the case of the EOF2s, we can notice a
500 long-period signal starting at the beginning of 2002-2003. The pattern coefficients of
501 EOF2s have opposite sign; this mode could be explained by invoking a variation in
502 gravity due to a height change resulting from a buoyancy effect and/or a soil
503 consolidation process. In this latter case, a decrease of the water content in the soil will
504 cause a height decrease which, in turn, will result into a gravity increase. The soil
505 consolidation phenomenon is known to occur particularly in clayey soils such as that
506 present at Medicina (Romagnoli et al., 2003).

### 7.3 GPS height and SG gravity

The EOF1s time components for MEDI and MSEL show a clear seasonal signal both in GPS heights and SG time series (Fig. 11a and b) as well as a long-period feature starting at the beginning of 2005. The pattern coefficients are of opposite sign (Table 10a and b), thus indicating anticorrelation between the two variables for the EOF1s. This means that the seasonal maxima and minima of GPS heights and SG gravity are opposite in phase as expected, and that, on a longer period of time, to the height increase starting in 2005 corresponds a gravity decrease. The EOF2s indicate the presence of a long-period oscillation with a minimum around 2002-2003. The pattern coefficients have the same sign (Table 10a and b) suggesting that this mode could result from buoyancy and/or soil consolidation effects.

## 8.0 Comparisons

We compared, as an example, the original detrended GPS height series and the reconstructed signals by means of the main EOFs components for the two cases A and B (see section 6.1). According to our arbitrary choice, the reconstructed signals must explain at least 70% of the observed variance. Therefore, three EOFs were used in case A, thus accounting for 70.2% of the variance (Table 2 and Fig. 12). In case B, five EOFs were selected which represent 78.9% of the variance (Table 3 and Fig. 13)**.** For the stations which are common to cases A and B, there are no major differences between the

two EOF reconstructions. However, it shall be noticed that in case A (Fig. 12) Marina di Ravenna shows, in the period 2004-2006 a minor discrepancy between the observed height residuals and the reconstructed signal, which does not appear in case B (Fig. 13). This difference might be due to the fact that the reconstruction of the signal in case B is accomplished through a slightly larger variance (78.9%) with respect to A (70.2 %). In case B, the analysis is also covering a larger area with respect to A; this might imply the presence of an additional regional component.

## 9.0 Conclusions

Over northeastern Italy, starting around 2004-2005, a reduction of the subsidence rates has been observed in conjunction with a decrease of the hydrological load on the Earth's crust mostly due to a decrease in the amount of precipitation.

The EOF and SVD analyses of the residuals of the GPS heights, hydrological parameters and gravity made it possible to identify long and short period oscillations and also to recognize common features in different pairs of variables. These findings, obtained by means of purely mathematical approaches, are supported by sound physical interpretation that allows to point at the local/regional hydrology as one of the main contributors to the observed height oscillations. Since a percentage of variance or covariance is associated to each EOF or SVD component respectively, the mathematical decomposition of the time series, together with the physical interpretation, provides a means to attribute a relative weight to the different phenomena involved.

552 In both the analyzed A and B cases (section 6.1), the time components of the main
553 EOFs show a slope inversion starting around 2004-2005. In particular, a coherent height
554 increase is found by EOF1 in case A (Fig. 6a, Table 2) and by EOF2 in case B (Fig. 6b,
555 Table 3). Also the EOF1 spatial pattern in case B clearly indicates an opposite north-
556 south behavior of the station heights on the short as well as on the multi-year period
557 (Table 3). For example, at seasonal scale, this means that summer height maxima of the
558 stations in the southern Po Plain are mirrored by height minima in the northern part of the
559 region. Case B, which involves a larger spatial domain with respect to case A, has made
560 it possible to recognize a regional signal.

561 As regards precipitation, the EOF1s of both the four and seven station cases
562 (section 6.2) show a marked decrease in the precipitation residuals starting at the end of
563 2005 (Fig. 7a and b and Tables 4 and 5).

564 The SVD analysis of the GPS heights and precipitation series has demonstrated
565 the high spatial covariance and the high time correlation between these two parameters.
566 The SVD1 in both analyses indicates that the GPS heights of the sites in the southern Po
567 Plain are anticorrelated with precipitation, while the northern sites are positively
568 correlated. We have interpreted anticorrelation as the loading/unloading effect on the
569 Earth's crust exerted by the increase/decrease in precipitation, which occurs in the period
570 2002-2005 and 2006-2008 respectively (Fig. 8). The reduction in the precipitation regime
571 observed, for example, from the end of 2005, unloads the crust and it turns into a height
572 increase particularly at the stations located in the southern Po Plain which are
573 characterized mostly by clayey soils.

574 The opposite response to hydrological loading of the southern and northern parts
575 of the region under investigation (see 6.1, case B and 6.4 “eight GPS and seven
576 precipitation stations”) results in a south-north height gradient, which turns out to be in
577 the order of 0.1 mm over a distance of about 100 km, by assuming a 1 mm homogeneous
578 increase of precipitation over the entire area. When observing and studying crustal
579 deformation of a region, it is important to identify how the height of the stations changes
580 in response to the hydrological load, in particular when weak tectonic signals are being
581 sought.

582 At Medicina, a few comparisons were made, namely between GPS heights and
583 water table, SG gravity data and hydrology and between GPS heights and SG gravity
584 (Fig. 10). In all three cases, the EOF1s time components are characterized by a clear
585 seasonal signal. This is due to loading/unloading of the crust in the case of the GPS
586 height variations and to variations of Newtonian mass attraction and height in the case of
587 gravity. GPS height and SG gravity show a marked common seasonal signal as well as a
588 long-term fluctuation (Fig. 11) pointing to a height increase which is quite evident
589 starting from the end of 2005.

590

591 **References**

592

593 Altamimi, Z., X. Collilieux, J. Legrand, B. Garayt and C. Boucher (2007), ITRF2005: A
594 new release of the International Terrestrial Reference Frame based on time series of
595 station positions and Earth Orientation Parameters, J. Geophys. Res., 112, B09401,
596 doi:10.1029/2007JB004949.

Björnsson, H. and S. Venegas (1997), A Manual for EOF and SVD Analyses of Climate Data. CCGCR Report No. 97-1, Montréal, 52 pp (available from www.awi.de).

Blewitt, G., D. Lavallée, P. Clarke and K. Nurutdinov (2001), A new global mode of Earth deformation: Seasonal cycle detected, Science, 294, 2342– 2345.

Bretherton, F. P., R. E. Davis, and C. B. Fandry (1976), A technique for objective analysis and design of oceanographic experiments applied to MODE-73, Deep-Sea Res., 23, 559–582.

Bretherton, C.S., C. Smith, and J.M. Wallace (1992), An intercomparison of methods for finding coupled patterns in climate data. J. Climate, 5, 541–560.

Carminati, E. and G. Di Donato, (1999), Separating natural and anthropogenic vertical movements in fast subsiding areas: the Po Plain (N. Italy) case. Geophys. Res. Lett. 26, 2291–2294.

Carminati, E. and G. Martinelli (2002), Subsidence rates in the Po Plain, northern Italy: the relative impact of natural and anthropogenic causation. Engineering Geology, 66, 241–255.

619 Carminati, E., C. Doglioni, and D. Scrocca (2003), Apennines subduction related
620 subsidence of Venice (Italy), Geophys. Res. Lett., 303(13), 1717,
621 doi:10.1029/2003GL017001.
622
623 Dach, R., U. Hugentobler, P. Fridez and M. Meindl (2007), Bernese GPS Software
624 version 5.0, Stämpfli Publications AG Bern, 612 pp.
625
626 Ferretti, A., C. Prati and F. Rocca (2001), Permanent Scatterers in SAR interferometry,
627 IEEE Trans Gars, 8-20.
628
629 Ferretti, A., T.R.E. (Tele-Rilevamento Europa T.R.E. srl) (2009), Private communication.
630
631 Gandin, L. S. (1965), Objective Analysis of Meteorological Fields, Israel Program for
632 Scientific Translations, 242 pp.
633
634 Hannachi, A. (2004), A Primer for the EOF Analysis of Climate Data, Department of
635 Meteorology, University of Reading, UK, 33pp (Available from: ncas-cms.nerc.ac.uk)
636
637 Hargreaves, G.H. and Z.A. Samani (1982), Estimating potential evapo-transpiration. J.
638 Irig and Drain Engr., ASCE, 108 (IR3), 223-230.
639
640 Hargreaves, G.H. and Z.A. Samani (1985), Reference crop evapo-transpiration from
641 temperature. Transactions of ASAE, 1 (2), 96-99.

642

643 Pignone, R., U. Cibin, P. Severi (2008), Pianura bolognese e costa le aree più critiche,
644 Supplemento al N. 1, anno XI, ARPA Rivista, gennaio-febbraio 2008, Il monitoraggio
645 della subsidenza - Esperienze a confronto, 8-9.

646

647 Romagnoli, C., S. Zerbini, L. Lago, B. Richter, D. Simon, F. Domenichini, C. Elmi, M.
648 Ghirotti (2003), Influence of soil consolidation and thermal expansion effects on height
649 and gravity variations, Journ. of Geodynamics, 35, N. 4-5, 521-539.

650

651 Szafranek, K. and A. Kenyeres (2009), Private communication.

652

653 Torge, W., (1989), Gravimetry, W. De Gruyter, 465 pp.

654

655 Van Dam, T.M., G. Blewitt, M.B. Heflin (1994), Atmospheric pressure loading effects on
656 Global Positioning System coordinate determinations, J. Geophys. Res., 99(B12), 23.939-
657 23.950.

658

659 van Dam, T. M., J. Wahr, P.C.D. Milly, A. B., Shmakin, G. Blewitt, D. Lavallèe and K.
660 M. Larson (2001), Crustal displacements due to continental water loading, Geophys. Res.
661 Lett., 28, 4, 651-654, doi: 10.1029/2000GL012120.

662

663 Vaníček, P. and E.J. Krakiwski (1986), Geodesy: the concepts, North-Holland,
664 Amsterdam, 697 pp.

Venegas, S.A. (2001) Statistical Methods for Signal Detection in Climate. DCESS Report No. 2, Niels Bohr Institute for Astronomy, Physics and Geophysics, University of Copenhagen, 96 pp.

von Storch, H., and A. Navarra (Eds.) (1999), Analysis of Climate Variability: Applications of Statistical Techniques, Springer Verlag, Berlin, 342 pp.

Zerbini, S., B. Richter, M. Negusini, D. Simon, C. Romagnoli and F. Domenichini (2000), Vertical crustal motions and mean sea level: an experiment in the Eastern Po Plain, in Land Subsidence, Proceedings of the Sixth International Symposium on Land Subsidence, 24-29 September 2000, Ravenna, Italy, L. Carbognin, G. Gambolati A.I. Johnson eds., ISBN 88-87222-06-1, vol. II, 151-163.

Zerbini S., M. Negusini, C. Romagnoli, F. Domenichini, B. Richter, D. Simon (2002), Multi-parameter continuous observations to detect ground deformation and to study environmental variability impacts, Global and Planetary Change 34, 37–58.

Zerbini S., B. Richter, F. Rocca, T. van Dam, F. Matonti, (2007), Combination of space and terrestrial geodetic techniques to monitor land subsidence: Case study, the southeastern Po Plain, Italy, Journ. Geophys. Res. Solid Earth, 112, B05401, doi:10.1029/2006JB004338.

**Acknowledgments**

This work has been developed in the frame of the IGCP 565 project “Developing the Global Geodetic Observing System into a Monitoring System for the Global Water Cycle”. The authors are grateful to Dr. Erika De Simone for having contributed to the analysis of the GPS data and to Dr. Hartmut Wziontek and Eng. Peter Wolf for the analysis of the SG gravity data. We would like to thank Prof. A. Ferretti and T.R.E. for having provided the InSAR results. We also would like to thank Drs. K. Szafranek. and A. Kenyeres for having provided the weekly EUREF GPS height solutions of the MEDI station. The authors are also grateful to two unknown reviewers the comments and suggestions of which helped us to improve the manuscript.

700 Figure Captions

701

702 Figure 1. Map of station locations in northeastern Italy. Bologna, Loiano, Marina di
703 Ravenna, Medicina (MSEL) are stations of the GPS network run by the University of
704 Bologna; Boretto belongs to Telespazio; Cavallino, Marghera, San Felice, Treviso and
705 Voltabarozzo are stations of the GPS network run by Consorzio Venezia Nuova for the
706 Magistrato alle Acque of Venice; the MEDI station belongs to the Italian Space Agency.

707

708 Figure 2. Medicina: daily water table (cyan line), hydrological balance (red line) and
709 precipitation (black line) data.

710

711 Figure 3. Time series of GPS heights and gravity; they are ordered from south to north.
712 Panel a) Loiano (LOIA) daily GPS height (purple line); b) Marina di Ravenna (RA)
713 daily GPS height (red line); c) Bologna (BOLG) daily GPS height (blue line) and a series
714 of AG measurements (red dots); d) Medicina GPS heights: MEDI (magenta line, EUREF
715 weekly solution) and MSEL (olive line, daily solution); daily SG time series (blue line)
716 and AG measurements (red dots); e) Boretto (BR) daily GPS height (dark yellow line); f)
717 San Felice (SF) daily GPS height (wine line); g) Voltabarozzo (VO) daily GPS height
718 (dark green line) and AG measurements (red dots); h) Marghera (MA) daily GPS height
719 (dark blue line) and AG measurements (red dots); i) Cavallino (CA) daily GPS height
720 (orange line) and AG measurements (red dots); j) Treviso (TV) daily GPS height (violet
721 line) and AG measurements (red dots). In all panels, gravity is multiplied by (-1).

722

723 Figure 4. InSAR maps of the terrain deformation in the Bologna area; (a) ERS
724 descending passes in the period 1992-2000 and (b) Radarsat descending passes during
725 2003-2007.
726
727 Figure 5. GPS height, precipitation (black line) and hydrological balance (cyan line)
728 residuals. GPS: Panel a): LOIA (purple line); b) RA (red line); c) BOLG (blue line); d)
729 MSEL (olive line) and MEDI (magenta line); e) BR (dark yellow line); f) SF (wine line);
730 g) VO (dark green line); h) MA (dark blue line); i) CA (orange line); j) TV (violet line).
731
732 Figure 6. EOF1 and EOF2 time components of GPS height residuals. Panel a) Five GPS
733 stations: MSEL, MEDI, RA, BOLG and BR; b) Eight GPS stations: MSEL, MEDI, RA,
734 BOLG, BR, CA, SF and VO.
735
736 Figure 7. EOF1 and EOF2 time components of precipitation residuals. Panel a) Four
737 precipitation stations: Medicina (ME), Marina di Ravenna (RA), Bologna (BO) and
738 Boretto (BR); b) Seven precipitation stations: ME, RA, BO, BR, Cavallino (CA), San
739 Felice (SF) and Voltabarozzo (VO).
740
741 Figure 8. SVD1 and SVD2 time components of the variable pair GPS height (blue dots)
742 and precipitation residuals (red dots). Panel a) Five GPS stations (MSEL, MEDI, RA,
743 BOLG and BR) and four precipitation stations (ME, RA, BO and BR); b) Eight GPS
744 stations (MSEL, MEDI, RA, BOLG, BR, CA, SF and VO) and seven precipitation
745 stations (ME, RA, BO, BR, CA, SF and VO).

746

747 Figure 9. EOF1 and EOF2 time components of the Medicina GPS height and water table
748 residuals. Panel a) MEDI and water table; b) MSEL and water table.

749

750 Figure 10. EOF1 and EOF2 time components of the Medicina superconducting
751 gravimeter (SG) and local hydrology residuals: Panel a) SG and precipitation; b) SG and
752 water table.

753

754 Figure 11. EOF1 and EOF2 time components of the Medicina GPS height and
755 superconducting gravimeter (SG) residuals. Panel a) MEDI and SG; b) MSEL and SG.

756

757 Figure 12. EOF reconstruction and observed height residuals. Five GPS stations: Panel a)
758 RA, observed height residuals (red line) and EOF reconstruction (green line); b) BOLG
759 (blue and purple); c) MSEL (olive and orange); d) MEDI (magenta and navy) and e) BR
760 (dark yellow and cyan). The reconstruction is based on the first three EOFs and explains
761 70.2% of the total variance.

762

763 Figure 13. EOF reconstruction and observed height residuals. Eight GPS stations: Panel
764 a) RA, observed height residuals (red line) and EOF reconstruction (green line); b)
765 BOLG (blue and purple); c) MSEL (olive and orange); d) MEDI (magenta and navy); e)
766 BR (dark yellow and cyan); f) SF (grey and pink); g) VO (wine and yellow) and h) CA
767 (dark cyan and black). The reconstruction is based on the first five EOFs and explains
768 78.9% of the total variance.

769

770 Table Captions

771

772 Table 1.

773 List of stations, North/South regional identifier, techniques available and linear trends of
774 the GPS height, Superconducting Gravimeter (SG) and Absolute Gravity (AG) series.
775 The formal error associated to the estimated trends, both for GPS heights and gravity,
776 have been multiplied by an arbitrary factor of 5 to provide conservative estimates of the
777 errors. The superscript (a) indicates that only one AG measurement is available at LOIA.
778 The superscript (b) indicates that the MEDI data are EUREF weekly solutions.

779

780 Table 2. EOF analysis of five GPS height residuals series (MSEL, MEDI, RA, BOLG
781 and BR). The second column lists the percentage of variance explained (PVE) by each
782 EOF, the following columns describe the spatial patterns.

783

784 Table 3. EOF analysis of eight GPS height residuals series (MSEL, MEDI, RA, BOLG,
785 BR, CA, SF and VO). The second column lists the percentage of variance explained
786 (PVE) by each EOF, the following columns describe the spatial patterns.

787

788 Table 4. EOF analysis of four precipitation residuals series (ME, RA, BO and BR). The
789 second column lists the percentage of variance explained (PVE) by each EOF, the
790 following columns describe the spatial patterns.

791

Table 5. EOF analysis of seven precipitation residuals series (ME, RA, BO, BR, CA, SF and VO). The second column lists the percentage of variance explained (PVE) by each EOF, the following columns describe the spatial patterns.

Table 6. SVD analysis of the variable pair GPS height (a) and precipitation residuals (b). Five GPS stations (MSEL, MEDI, RA, BOLG and BR) and four precipitation stations (ME, RA, BO and BR). The two stations at Medicina, MSEL and MEDI, are coupled to the same ME precipitation data series. The second column lists the squared covariance percentage relevant to each SVD, the following columns describe the spatial patterns.

Table 7. SVD analysis of the variable pair GPS height (a) and precipitation residuals (b). Eight GPS stations (MSEL, MEDI, RA, BOLG, BR, CA, SF and VO) and seven precipitation stations (ME, RA, BO, BR, CA, SF and VO). The two stations at Medicina, MSEL and MEDI, are coupled to the same ME precipitation data series. The second column lists the squared covariance percentage relevant to each SVD, the following columns describe the spatial patterns.

Table 8. EOF analysis of two time series, GPS height and water table residuals, at Medicina. The second column lists the percentage of variance explained (PVE) by each EOF, the following columns describe the spatial patterns. (a) MSEL and water table; (b) MEDI and water table.

814 Table 9. EOF analysis of two time series, superconducting gravimeter (SG) and local
815 hydrology residuals, at Medicina. The second column lists the percentage of variance
816 explained (PVE) by each EOF, the following columns describe the spatial patterns. (a)
817 SG and precipitation; (b) SG and water table.
818
819 Table 10. EOF analysis of two time series, GPS height and superconducting gravimeter
820 (SG) residuals, at Medicina. The second column lists the percentage of variance
821 explained (PVE) by each EOF, the following columns describe the spatial patterns. (a)
822 MEDI and SG; (b) MSEL and SG.

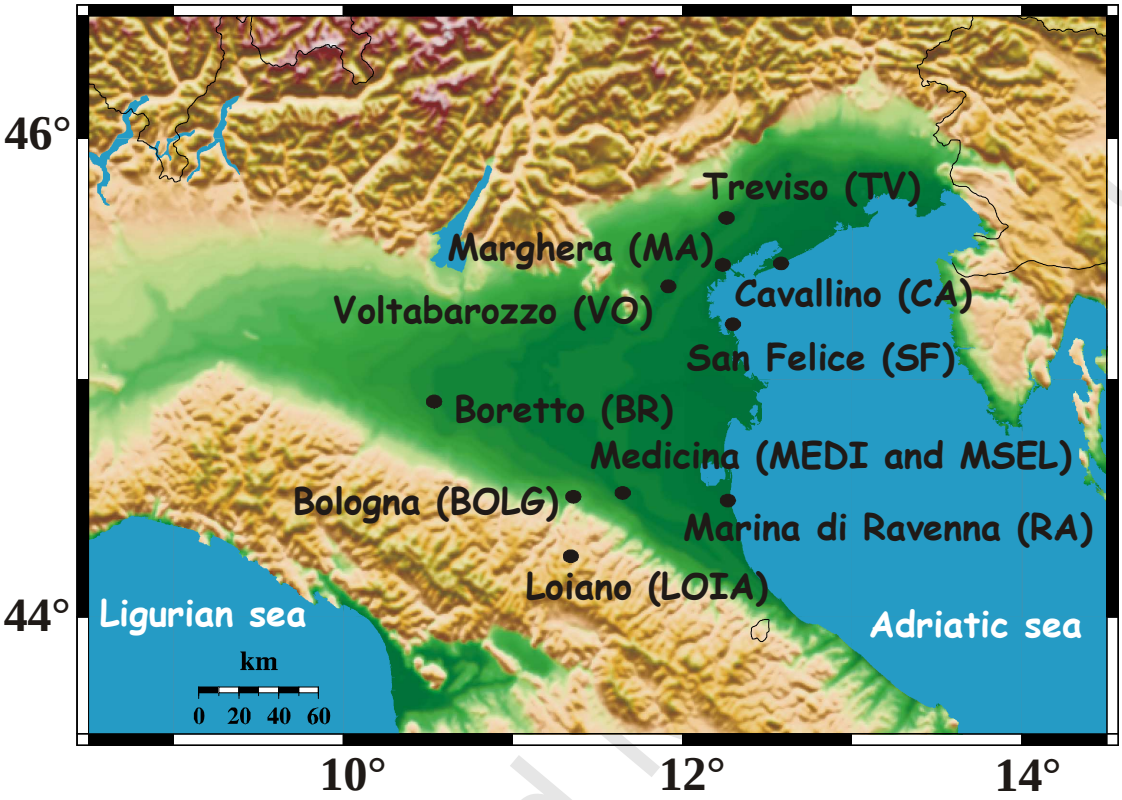


Figure 1

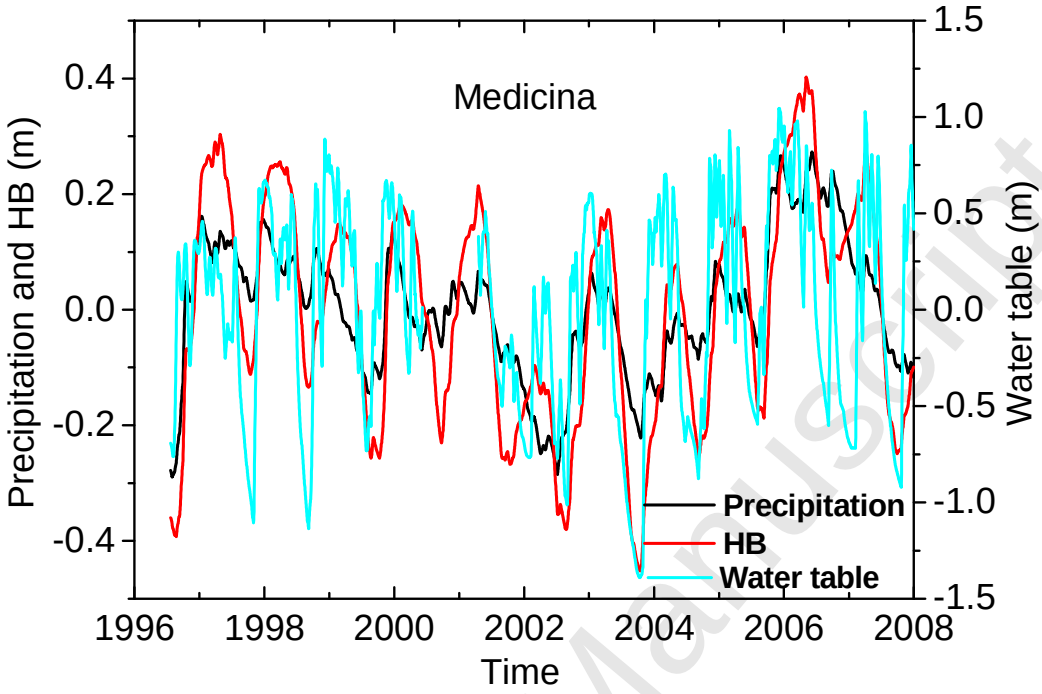


Figure 2

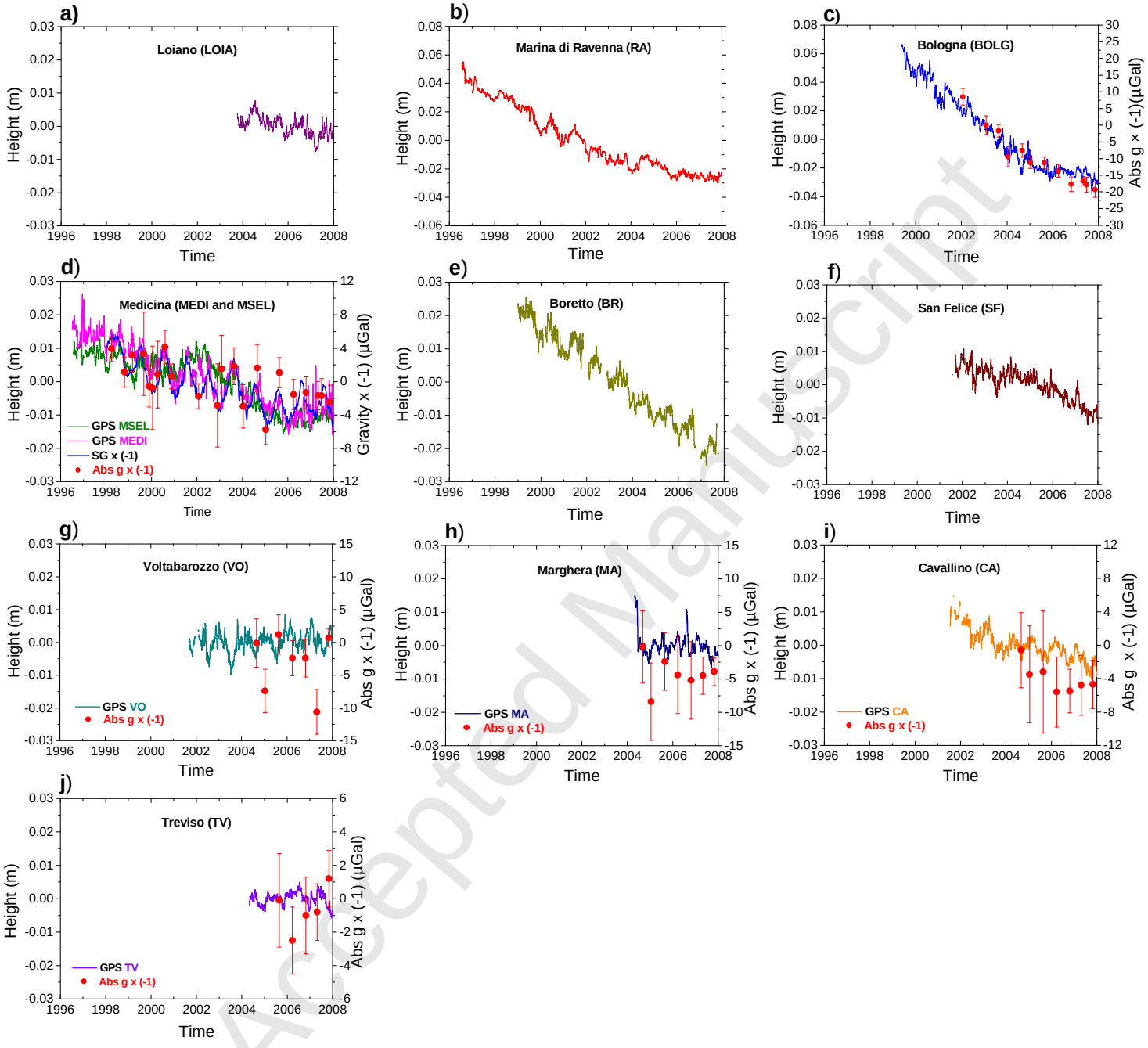


Figure 3

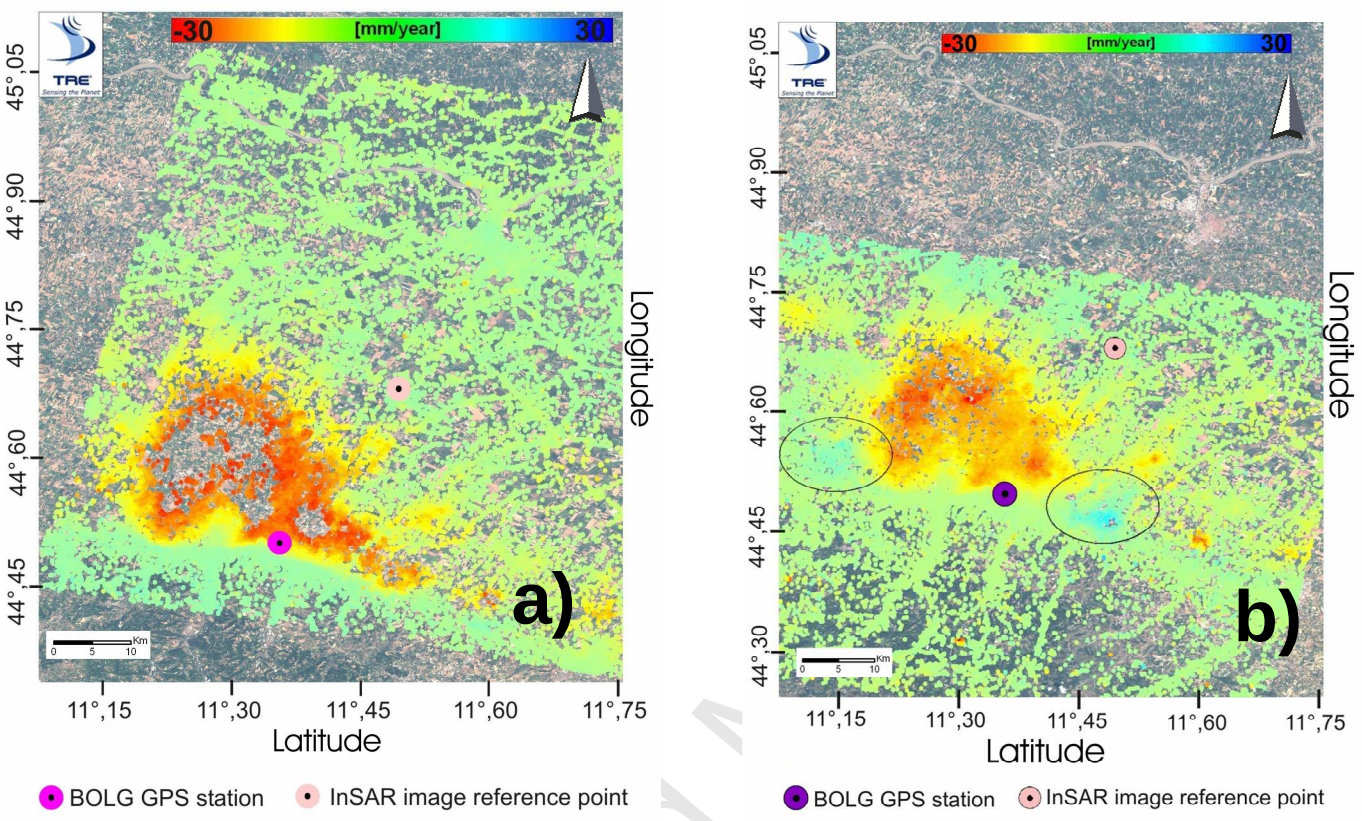


Figure 4

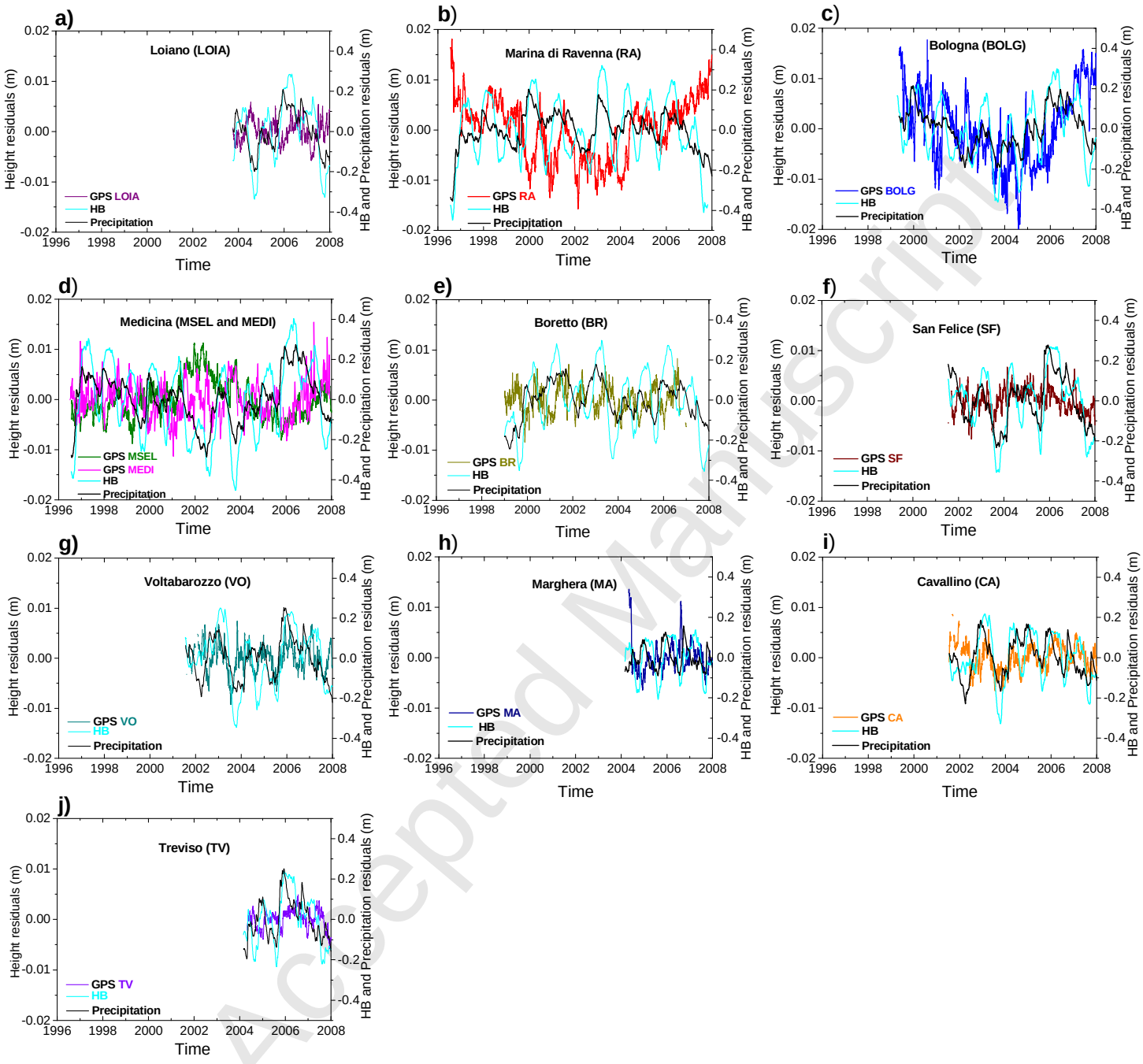


Figure 5

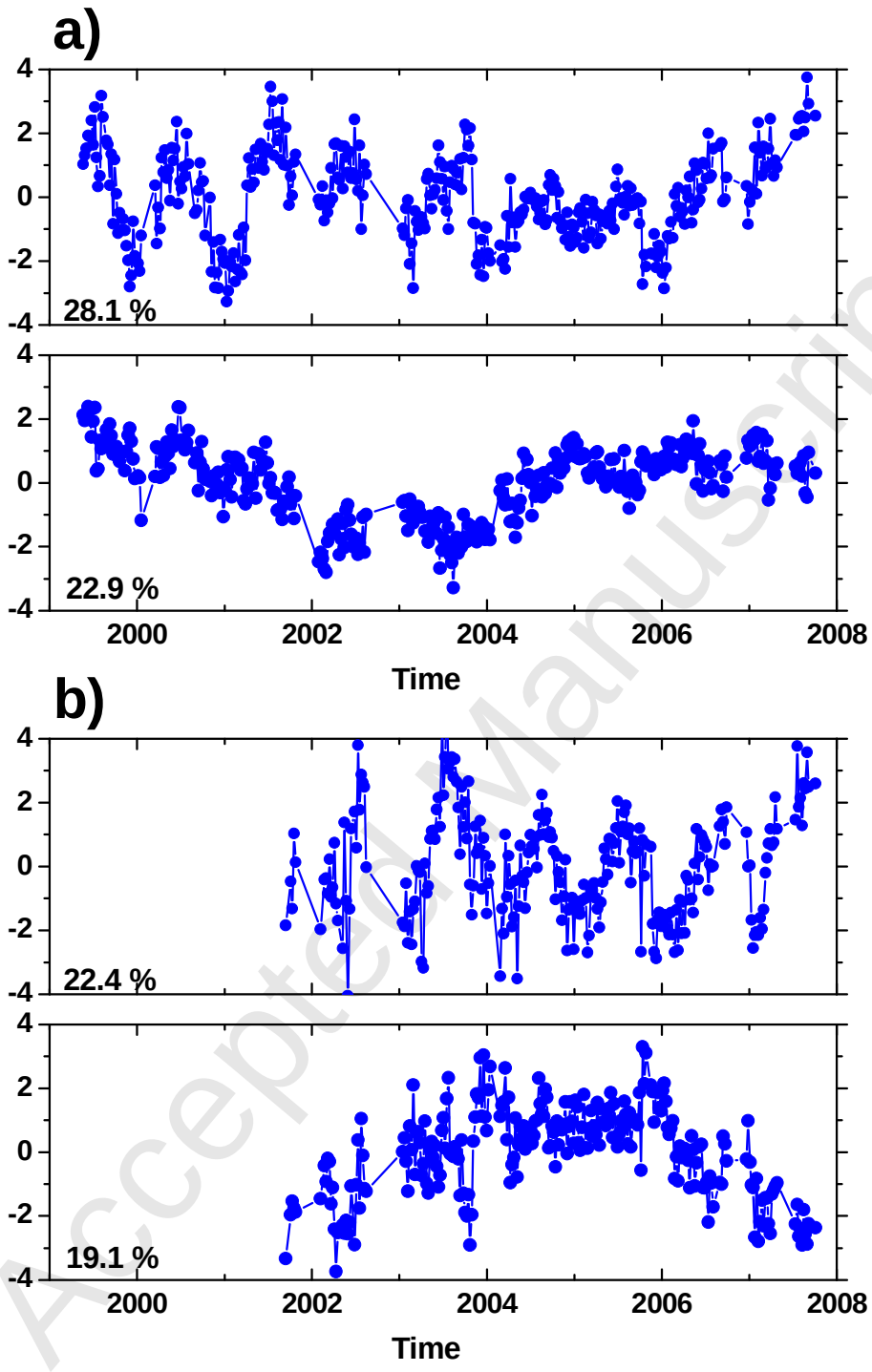


Figure 6

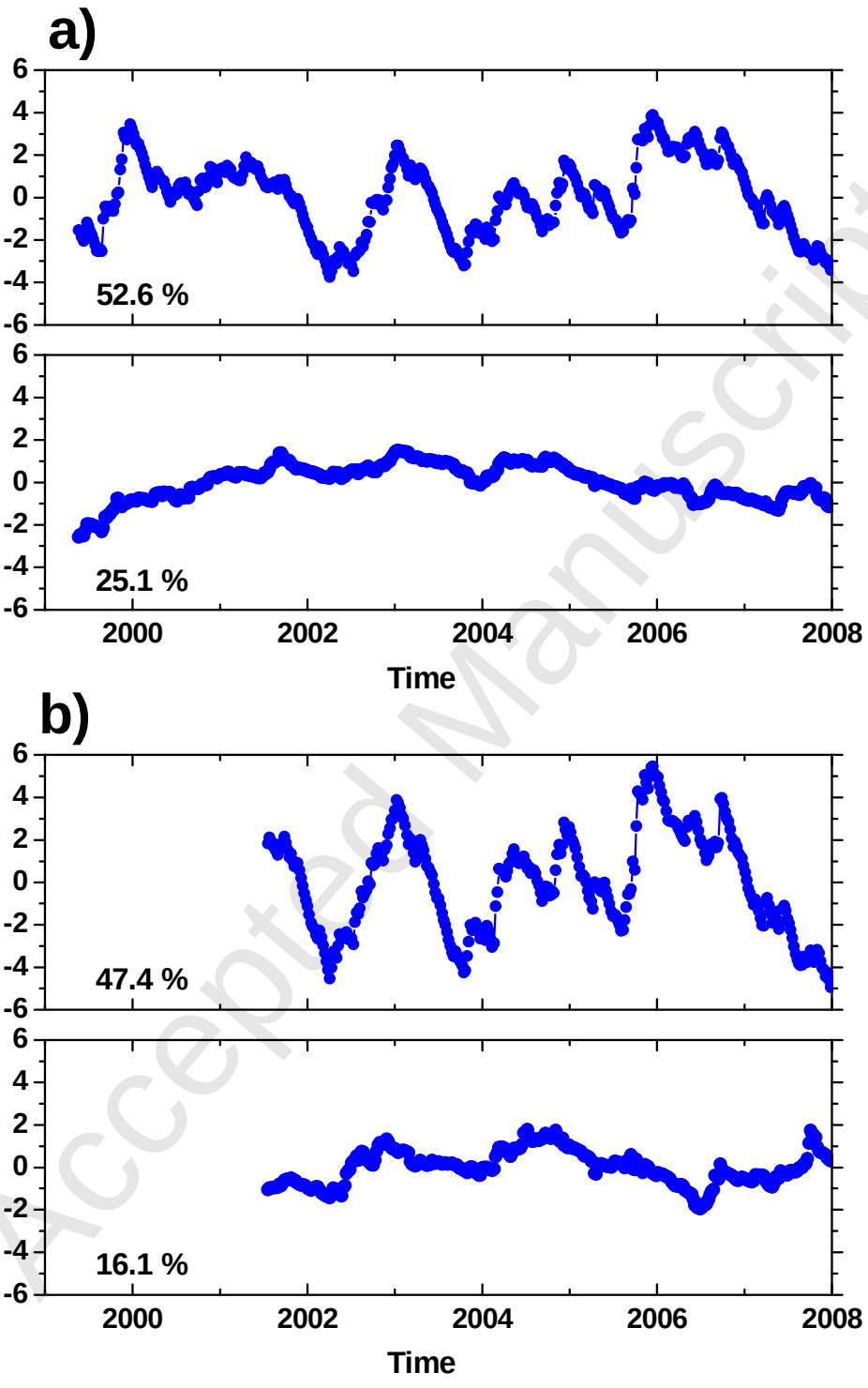


Figure 7

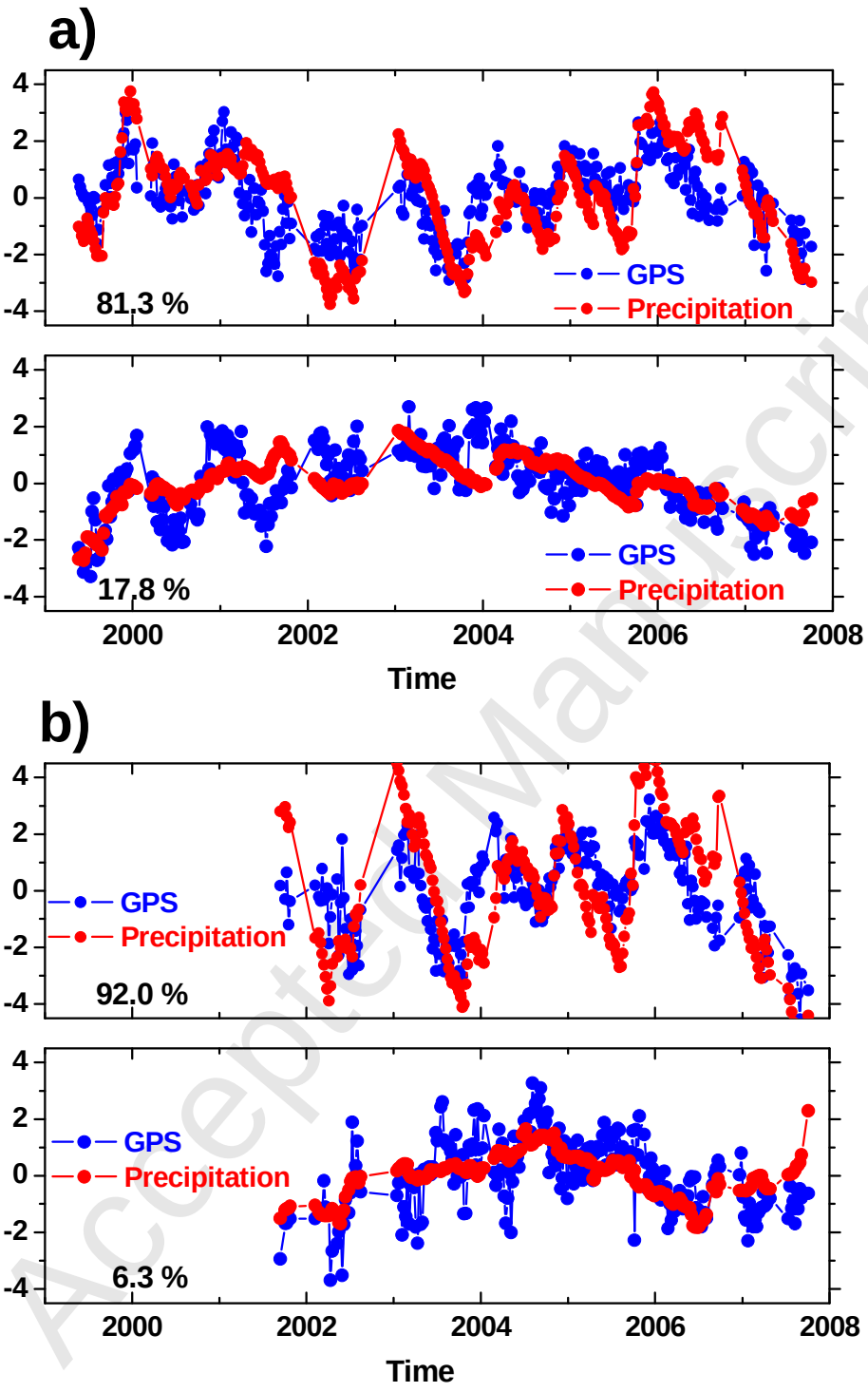


Figure 8

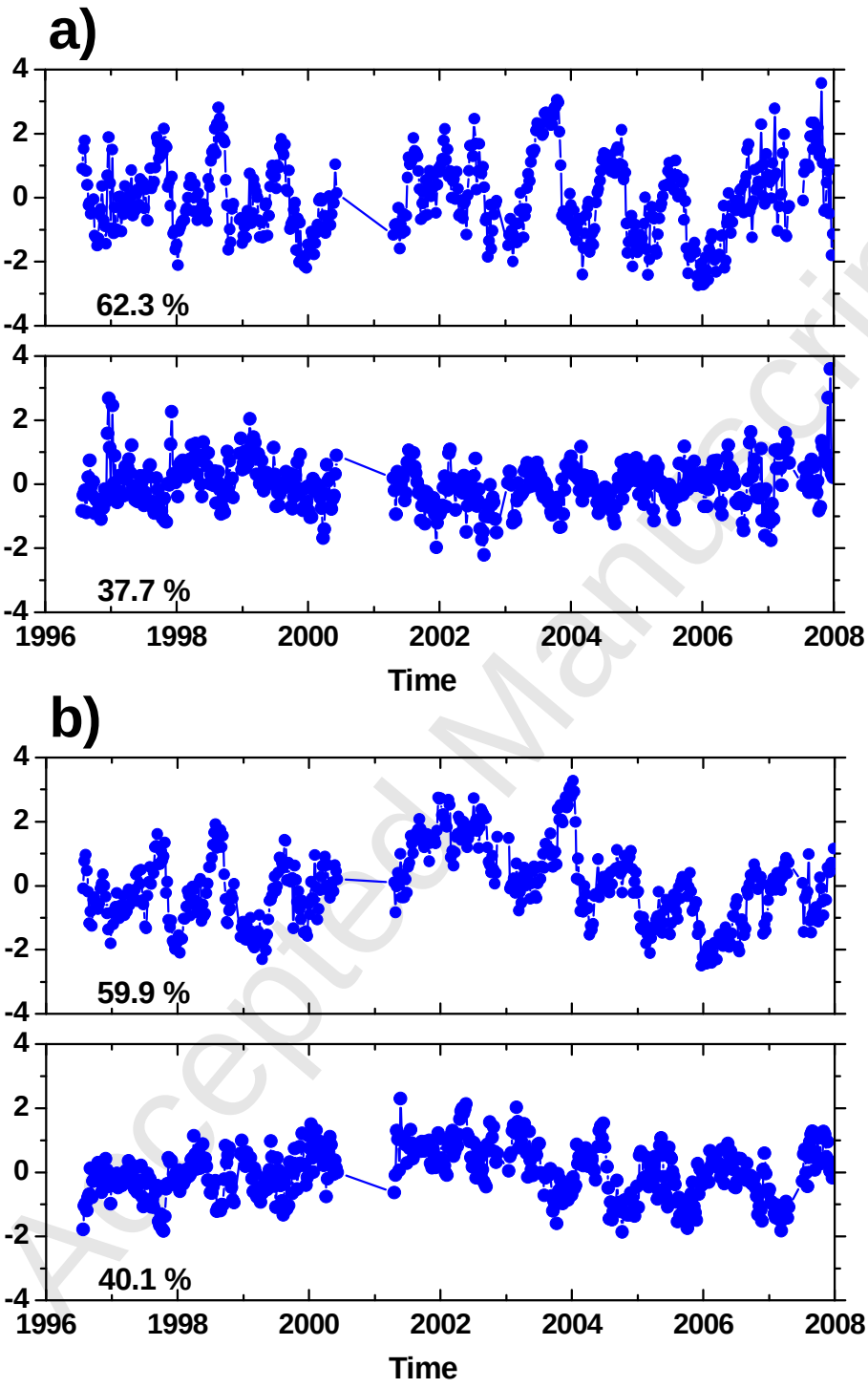


Figure 9

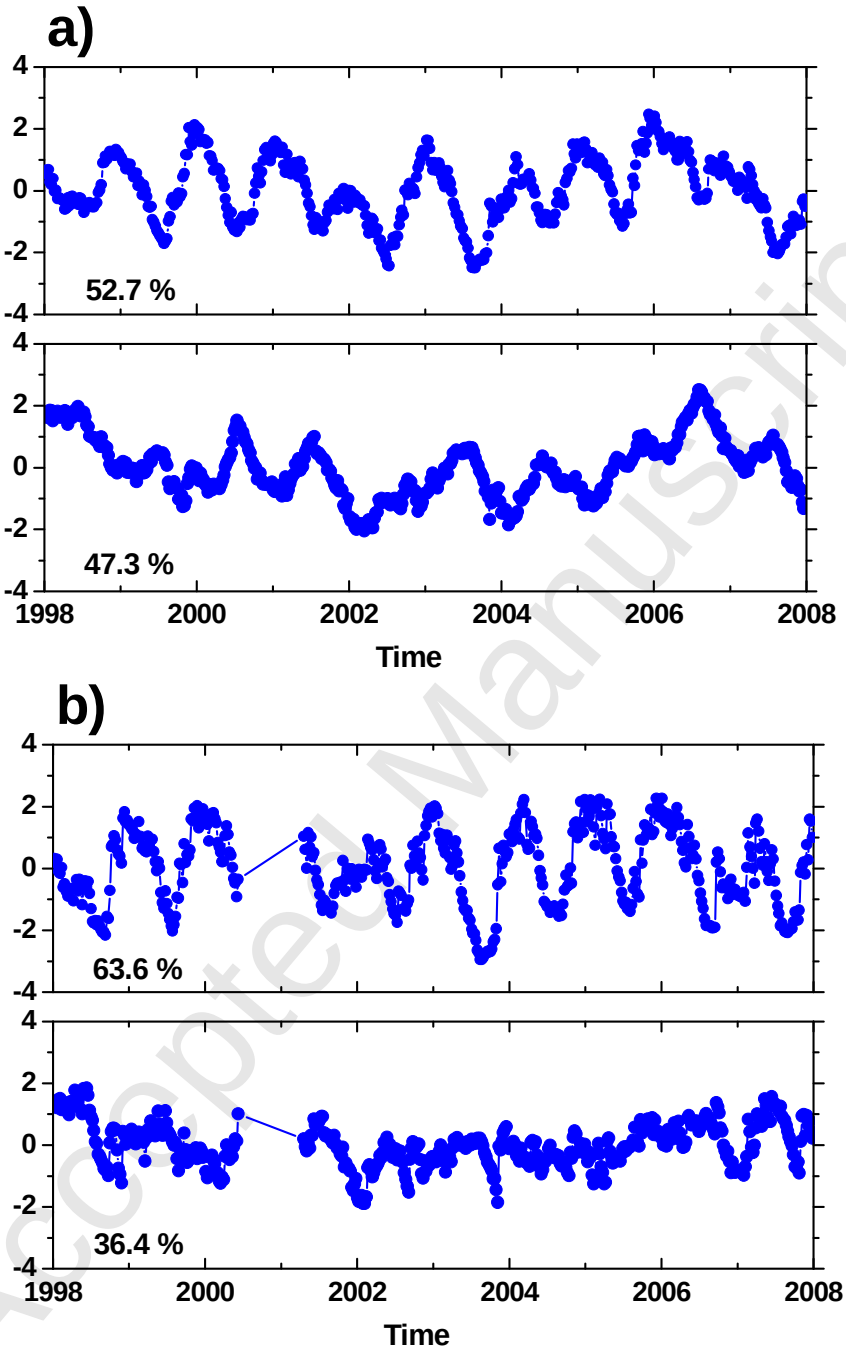


Figure 10

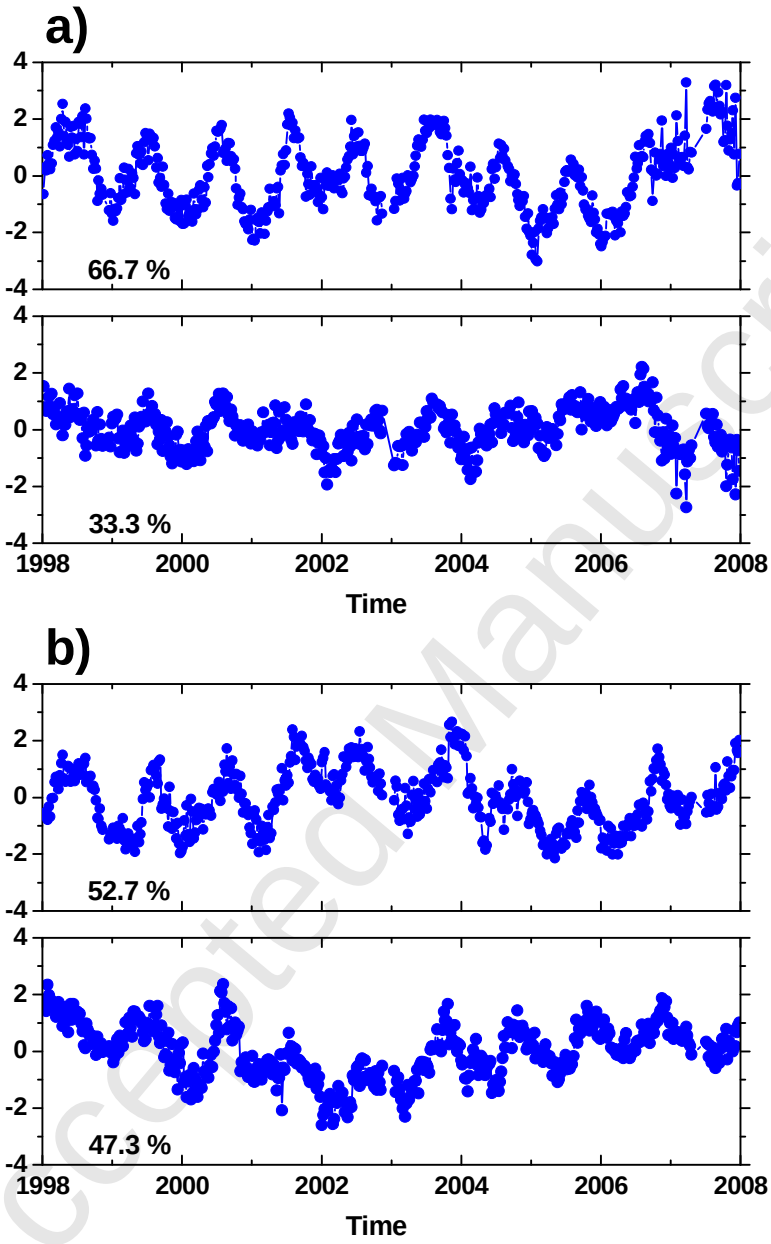


Figure 11

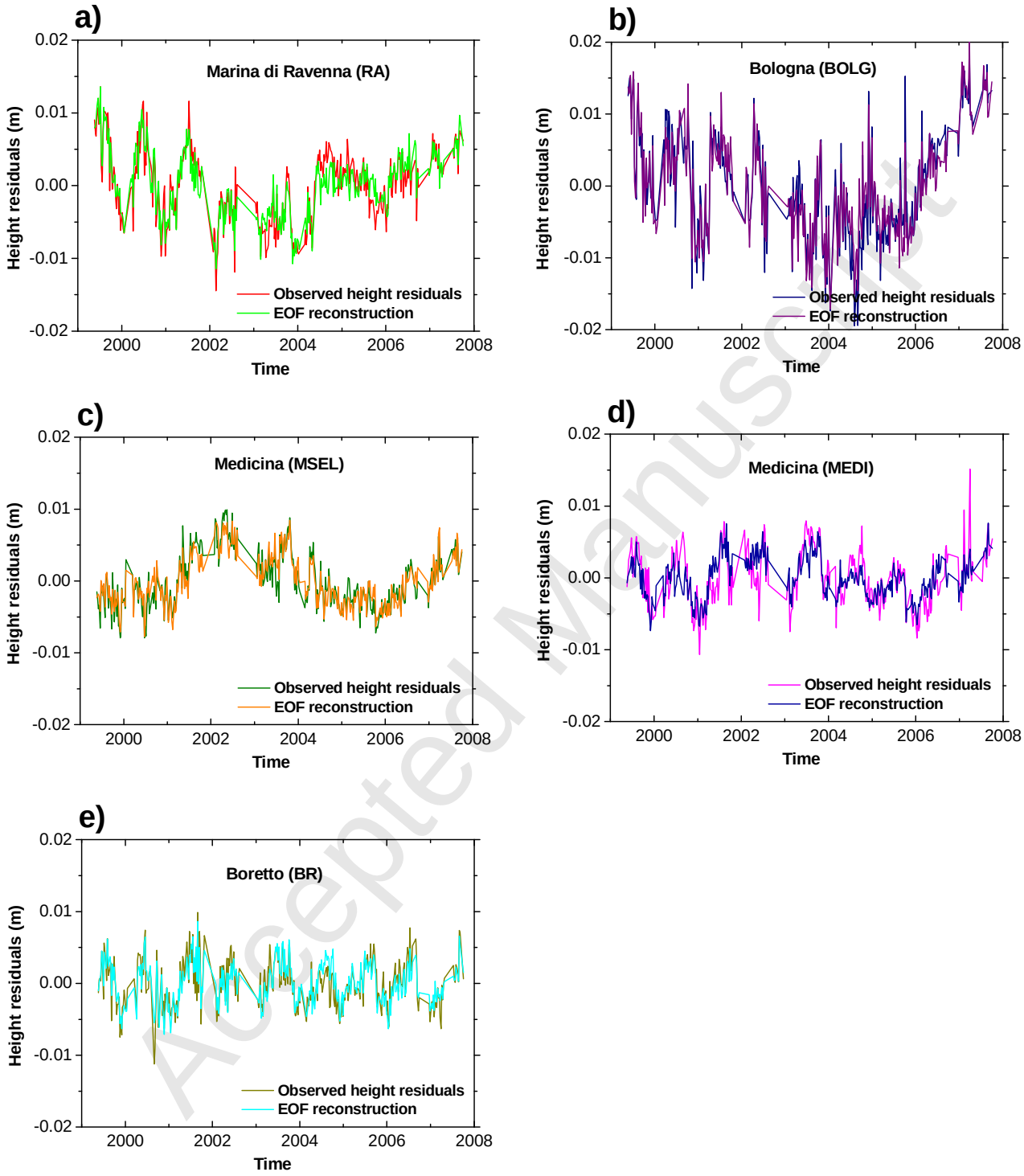


Figure 12

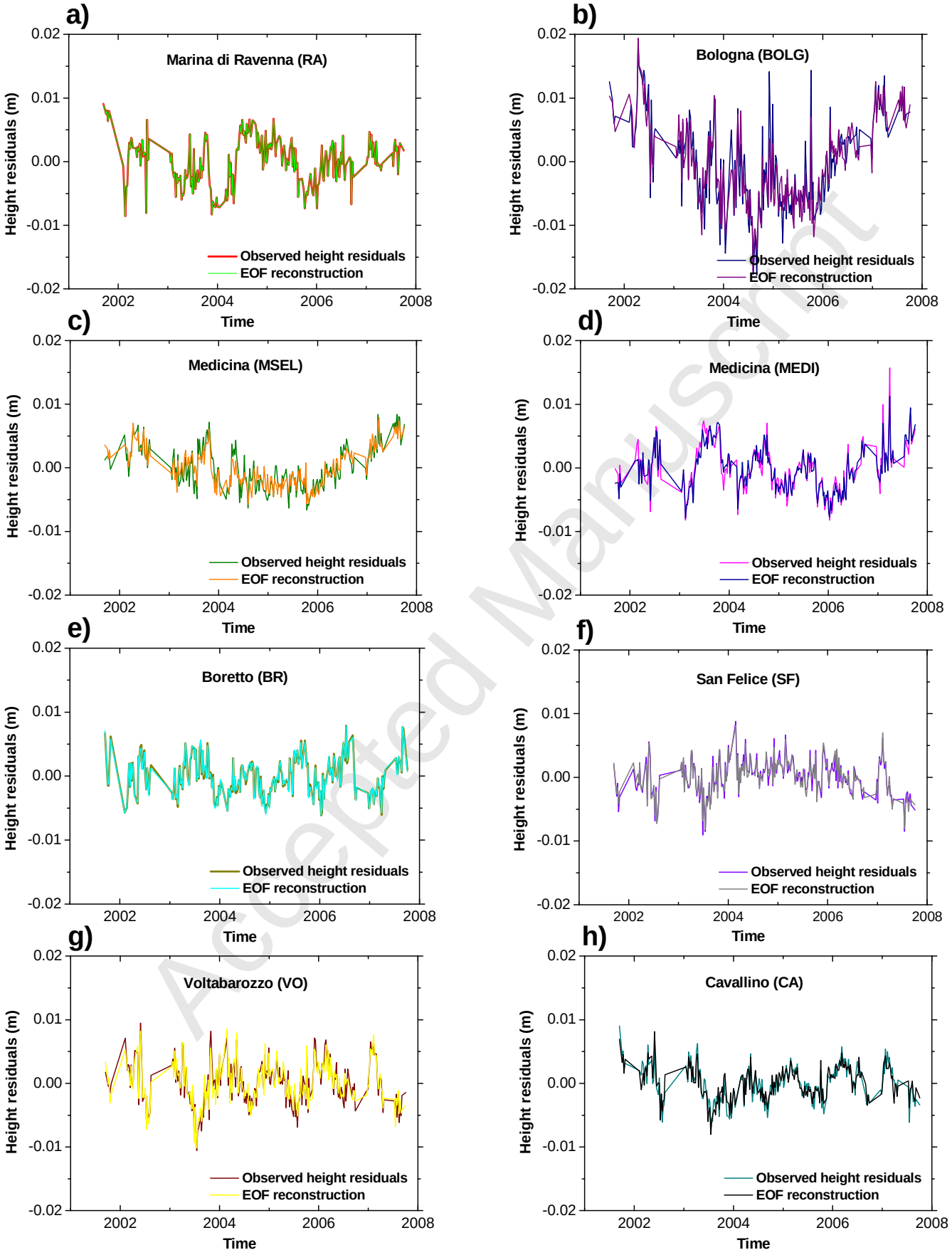


Figure 13

Table 1.

| Station name | North/South | Technique | Linear trend (mm/yr) GPS (μGal/yr) SG, AG |
|---|---|---|---|
| Loiano [(a)] (LOIA) | S | GPS | -1.41±0.25 |
| | | AG | --------- |
| Marina di Ravenna (RA) | S | GPS | -6.51±0.15 |
| Bologna (BOLG) | S | GPS | -10.57±0.25 |
| | | AG | +4.17±1.75 |
| Medicina (Gravity) | S | SG | +0.71±0.05 |
| | | AG | +0.52±0.65 |
| Medicina [(b)] (MEDI) | S | GPS | -2.44±0.25 |
| Medicina (MSEL) | S | GPS | -2.13±0.10 |
| Boretto (BR) | S | GPS | -5.00±0.10 |
| San Felice (SF) | N | GPS | -2.24±0.15 |
| Voltabarozzo (VO) | N | GPS | +0.36±0.15 |
| | | AG | -0.98±1.07 |
| Marghera (MA) | N | GPS | -0.88±0.40 |
| | | AG | -0.88±1.41 |
| Cavallino (CA) | N | GPS | -1.97±0.15 |
| | | AG | +0.29±1.46 |
| Treviso (TV) | N | GPS | 0.00±0.25 |
| | | AG | -1.64±1.50 |

Table 10

(a)

| EOF | PVE | MEDI | SG |
|---|---|---|---|
| 1 | 66.7 | +0.71 | -0.71 |
| 2 | 33.3 | -0.71 | -0.71 |

(b)

| EOF | PVE | MSEL | SG |
|---|---|---|---|
| 1 | 52.7 | +0.71 | -0.71 |
| 2 | 47.3 | -0.71 | -0.71 |

Table 2

| EOF | PVE | GPS spatial pattern | | | | |
|---|---|---|---|---|---|---|
| | | MSEL | MEDI | RA | BOLG | BR |
| 1 | 28.1 | +0.38 | +0.50 | +0.43 | +0.44 | +0.47 |
| 2 | 22.9 | -0.62 | -0.29 | +0.62 | +0.37 | -0.10 |
| 3 | 19.2 | +0.36 | -0.08 | -0.17 | +0.64 | -0.65 |
| 4 | 17.1 | -0.25 | +0.76 | +0.16 | -0.25 | -0.52 |
| 5 | 12.6 | -0.53 | +0.29 | -0.61 | +0.44 | +0.27 |

Table 3

| EOF | PVE | GPS spatial pattern | | | | | | | |
|---|---|---|---|---|---|---|---|---|---|
| | | MSEL | MEDI | RA | BOLG | BR | CA | SF | VO |
| 1 | 22.4 | +0.12 | +0.41 | +0.03 | -0.13 | +0.22 | -0.47 | -0.48 | -0.54 |
| 2 | 19.1 | -0.60 | -0.26 | -0.26 | -0.59 | -0.24 | -0.26 | +0.07 | -0.13 |
| 3 | 14.5 | +0.22 | +0.08 | -0.70 | +0.30 | -0.53 | -0.19 | -0.18 | +0.10 |
| 4 | 11.8 | +0.01 | +0.14 | +0.62 | -0.01 | -0.76 | -0.08 | -0.07 | -0.03 |
| 5 | 11.1 | -0.05 | -0.66 | +0.06 | +0.20 | -0.03 | +0.26 | -0.62 | -0.25 |
| 6 | 8.2 | -0.66 | +0.50 | -0.09 | +0.31 | -0.02 | +0.42 | -0.18 | -0.07 |
| 7 | 6.9 | +0.36 | +0.20 | -0.18 | -0.57 | -0.15 | +0.64 | -0.10 | -0.18 |
| 8 | 5.9 | -0.04 | +0.12 | +0.07 | -0.27 | +0.11 | -0.09 | -0.55 | +0.76 |

Table 4

| EOF | PVE | Precipitation spatial pattern | | | |
|---|---|---|---|---|---|
| | | ME | RA | BO | BR |
| 1 | 52.6 | +0.55 | +0.50 | +0.49 | +0.46 |
| 2 | 25.1 | -0.29 | +0.38 | -0.63 | +0.61 |
| 3 | 15.9 | +0.07 | -0.77 | +0.11 | +0.62 |
| 4 | 6.5 | -0.78 | +0.14 | +0.59 | +0.15 |

Table 5

| EOF | PVE | Precipitation spatial pattern | | | | | | |
|---|---|---|---|---|---|---|---|---|
| | | ME | RA | BO | BR | CA | SF | VO |
| 1 | 47.4 | +0.40 | +0.36 | +0.37 | +0.41 | +0.32 | +0.39 | +0.39 |
| 2 | 16.1 | -0.30 | +0.09 | -0.50 | +0.03 | +0.78 | -0.13 | +0.16 |
| 3 | 13.1 | +0.21 | +0.79 | -0.04 | -0.10 | 0.00 | -0.35 | -0.45 |
| 4 | 7.6 | -0.07 | +0.33 | -0.45 | -0.41 | -0.26 | +0.65 | +0.18 |
| 5 | 6.3 | 0.00 | -0.19 | +0.14 | -0.02 | +0.35 | +0.52 | -0.74 |
| 6 | 5.8 | -0.05 | +0.01 | +0.52 | -0.78 | +0.29 | -0.08 | +0.19 |
| 7 | 3.7 | +0.84 | -0.31 | -0.35 | -0.23 | +0.12 | -0.10 | +0.01 |

Table 6

(a)

| SVD | SCP | GPS spatial pattern | | | | |
|---|---|---|---|---|---|---|
| | | MSEL | MEDI | RA | BOLG | BR |
| 1 | 81.3 | -0.64 | -0.72 | -0.01 | +0.05 | -0.27 |
| 2 | 17.8 | +0.24 | -0.21 | -0.59 | -0.73 | -0.11 |
| 3 | 0.8 | -0.72 | +0.52 | -0.05 | -0.38 | +0.24 |
| 4 | 0.0 | -0.13 | +0.31 | -0.68 | +0.48 | -0.43 |

(b)

| SVD | SCP | Precipitation spatial pattern | | | |
|---|---|---|---|---|---|
| | | ME | RA | BO | BR |
| 1 | 81.3 | +0.59 | +0.46 | +0.56 | +0.36 |
| 2 | 17.8 | -0.26 | +0.64 | -0.56 | +0.47 |
| 3 | 0.8 | +0.23 | +0.53 | -0.17 | -0.80 |
| 4 | 0.0 | -0.73 | +0.32 | +0.59 | -0.13 |

Table 7

(a)

| SVD | SCP | GPS spatial pattern | | | | | | | |
|---|---|---|---|---|---|---|---|---|---|
| | | MSEL | MEDI | RA | BOLG | BR | CA | SF | VO |
| 1 | 92.0 | -0.55 | -0.59 | -0.13 | -0.19 | -0.20 | +0.34 | +0.25 | +0.28 |
| 2 | 6.3 | -0.36 | +0.23 | +0.20 | -0.62 | -0.19 | -0.52 | +0.19 | -0.23 |
| 3 | 1.3 | +0.03 | +0.05 | -0.95 | -0.18 | +0.16 | -0.16 | +0.02 | -0.08 |
| 4 | 0.2 | +0.03 | -0.36 | -0.08 | +0.40 | -0.45 | -0.67 | -0.16 | +0.16 |
| 5 | 0.1 | -0.64 | +0.17 | -0.07 | +0.35 | -0.02 | +0.11 | -0.45 | -0.46 |
| 6 | 0.1 | +0.20 | +0.27 | -0.15 | +0.09 | -0.77 | +0.32 | +0.29 | -0.26 |
| 7 | 0.0 | +0.25 | -0.59 | +0.07 | -0.04 | +0.14 | -0.02 | +0.14 | -0.74 |

(b)

| SVD | SCP | Precipitation spatial pattern | | | | | | |
|---|---|---|---|---|---|---|---|---|
| | | ME | RA | BO | BR | CA | SF | VO |
| 1 | 92.0 | +0.39 | +0.39 | +0.38 | +0.37 | +0.39 | +0.39 | +0.33 |
| 2 | 6.3 | -0.22 | +0.24 | -0.50 | -0.19 | +0.76 | -0.16 | +0.06 |
| 3 | 1.3 | +0.24 | +0.58 | +0.29 | -0.45 | -0.15 | -0.54 | +0.01 |
| 4 | 0.2 | -0.46 | -0.35 | +0.54 | -0.23 | +0.21 | -0.14 | +0.51 |
| 5 | 0.1 | +0.45 | -0.36 | -0.16 | +0.39 | +0.09 | -0.63 | +0.29 |
| 6 | 0.1 | -0.13 | -0.06 | +0.44 | +0.30 | +0.35 | -0.27 | -0.71 |
| 7 | 0.0 | -0.56 | +0.43 | -0.09 | +0.57 | -0.28 | -0.22 | +0.20 |

Table 8

(a)

| EOF | PVE | MEDI | WT |
|---|---|---|---|
| 1 | 62.3 | +0.71 | -0.71 |
| 2 | 37.7 | +0.71 | +0.71 |

(b)

| EOF | PVE | MSEL | WT |
|---|---|---|---|
| 1 | 59.9 | +0.71 | -0.71 |
| 2 | 40.1 | +0.71 | +0.71 |

Table 9

(a)

| EOF | PVE | Prec. | SG |
|---|---|---|---|
| 1 | 52.7 | +0.71 | +0.71 |
| 2 | 47.3 | +0.71 | -0.71 |

(b)

| EOF | PVE | WT | SG |
|---|---|---|---|
| 1 | 63.6 | +0.71 | +0.71 |
| 2 | 36.4 | +0.71 | -0.71 |